Neurochemistry International 128 (2019) 21–31

Contents lists available at ScienceDirect

Neurochemistry International

journal homepage: www.elsevier.com/locate/neuint

Pharmacological HIF inhibition prevents retinal neovascularization with improved visual function in a murine oxygen-induced retinopathy model

Yukihiro Miwa[a,b], Yusuke Hoshino[a], Chiho Shoda[a,b,c], Xiaoyan Jiang[a,b], Kazuo Tsubota[b,**], Toshihide Kurihara[a,b,*]

[a] Laboratory of Photobiology, Keio University School of Medicine, Tokyo, Japan
[b] Department of Ophthalmology, Keio University School of Medicine, Tokyo, Japan
[c] Department of Ophthalmology, Nihon University School of Medicine, Tokyo, Japan

A B S T R A C T

Neovascular retinal diseases are the leading causes of blindness in advanced countries. To date, anti-VEGF (vascular endothelial growth factor) drugs are clinically effective and widely used for these diseases. However, recent animal and clinical studies reported that potent and long-term VEGF antagonism may induce chorioretinal atrophy. Thus, physiological amount of VEGF is required for the homeostasis in the retina. Hypoxia-inducible factors (HIFs) are transcription factors located upstream of VEGF. We hypothesized that ectopically stabilized HIFs induce pathological amount of VEGF involved with retinal neovascularization. Therefore, HIF inhibition could be an alternative therapeutic candidate targeting the pathological amount of VEGF while holding a physiological amount of VEGF. To test this hypothesis, topotecan and doxorubicin, HIF inhibitors with different mechanisms were administered to the murine oxygen-induced retinopathy (OIR) model. We found that both topotecan and doxorubicin significantly prevented pathological but not physiological neovascularization in OIR. Furthermore, impaired visual function observed in OIR can also be suppressed by administering topotecan. These data suggested that HIF inhibition may be effective for pathological angiogenesis and neurodegeneration of the retina.

1. Introduction

Abnormal blood vessel growth in the retina is a common feature of many eye diseases such as retinopathy of prematurity (ROP), age-related macular degeneration (AMD), and diabetic retinopathy (DR) (de Jong, 2006; Uddin et al., 2016). These diseases are major leading causes of blindness in developed countries (Ding and Wong, 2012; Resnikoff et al., 2004). The pathological angiogenesis in these diseases is mainly induced by vascular endothelial growth factor (VEGF) (Aiello et al., 1995; Ferrara and Kerbel, 2005). As a treatment for this pathological angiogenesis, intravitreal anti-VEGF therapy is currently widely used (Pieramici and Rabena, 2008). However, to date, adverse effects such as neurodegeneration of the pan-VEGF blockade in the eye are well recognized (Cheung et al., 2014; Comparison of Age-related Macular Degeneration Treatments Trials Research et al., 2016; Grunwald et al., 2014; Lains et al., 2014). Therefore, there is a need for a novel approach which suppresses a pathological amount of VEGF without reducing a physiological amount of VEGF.

VEGF is regulated by several factors such as hypoxia-inducible factors (HIFs), transforming growth factor-β (TGF-β), insulin-like growth factor-1(IGF-1) and platelet-derived growth factor (PDGF) (Ferrara et al., 2003). In this study, we focused on HIFs that contribute to the pathological angiogenesis. HIFs play a critical role in cellular oxygen homeostasis (Wang and Semenza, 1995). Under a normoxic condition, α subunits of HIFs (HIF-αs) are constitutively hydroxylated by prolyl hydroxylase, ubiquitinated by von Hippel-Lindau protein (VHL), and degraded in a proteasome-dependent manner. Under a hypoxic condition, the activity of HIFα prolyl-hydroxylase decreases resulting in the HIFα stabilization (Kaelin and Ratcliffe, 2008). Then HIF-αs translocate to the nucleus, bind to hypoxia response element (HRE), and activate HIF target genes such as VEGF, BCL2 interacting protein 3 (BNIP3), and phosphoinositide-dependent kinase 1 (PDK1) (Mole et al., 2009). Our hypothesis is that HIF inhibition could prevent the pathological amount of VEGF while holding a physiological amount of VEGF.

In this study, we used two HIF inhibitors topotecan and doxorubicin with different mechanisms. Topotecan suppresses the accumulation of HIF-1α protein but not mRNA expression (Rapisarda et al., 2004; Yu et al., 2017). The effect of topotecan on HIF-2α is still unknown (Rapisarda et al., 2004). Doxorubicin is known to inhibit HIF-αs by blocking its binding to the hypoxia-response element (Yu et al., 2017).

The murine oxygen-induced retinopathy (OIR) model is a retinal proliferative vascular disease model developing neovascular tufts and

* Corresponding author. Laboratory of Photobiology, Department of Ophthalmology, Keio University School of Medicine; 35 Shinanomachi, Shinjuku-ku, Tokyo, 160-8582, Japan.
** Corresponding author. Department of Ophthalmology, Keio University School of Medicine; 35 Shinanomachi, Shinjuku-ku, Tokyo, 160-8582, Japan.
E-mail addresses: tsubota@z3.keio.jp (K. Tsubota), kurihara@z8.keio.jp (T. Kurihara).

https://doi.org/10.1016/j.neuint.2019.03.008
Received 30 November 2018; Received in revised form 26 February 2019; Accepted 8 March 2019
Available online 11 March 2019
0197-0186/

vaso-obliteration area (Connor et al., 2009). This model has been widely used for neovascular retinal diseases (Smith et al., 1994). The expression of HIF-αs and VEGF is known to be increased in the OIR model (Ozaki et al., 1999). In this study, we investigated the effect of HIF inhibition on the pathological angiogenesis and impaired visual function in OIR.

2. Material and methods

2.1. Animals

All procedures were approved by the Ethics Committee on Animal Research of the Keio University School of Medicine adhered to the ARVO Statement for the Use of Animals in Ophthalmic and Vision Research, the Institutional Guidelines on Animal Experimentation at Keio University, and the Animal Research: Reporting of In Vivo Experiments (ARRIVE) guidelines for the use of animals in research. C57BL/6 J mice were obtained from CLEA Japan, Inc.

2.2. Oxygen-induced retinopathy model and drug administration

Postnatal day 8 (P8) mice with their nursing mothers were exposed to hyperoxia (85%) for 72 h in an oxygen supply chamber. After oxygen exposure, mice were placed back in room air until P17 (Fig. 1A) (Okabe et al., 2014). Mice received intraperitoneal administration of topotecan (1.25 mg/kg, Cayman Chemical, Ann Arbor, MI, USA) (Guichard et al., 2001) or PBS once a day between P12 and P16. Mice received intraperitoneal administration of doxorubicin (1 mg/kg, Tokyo Chemical Industry Co., Ltd., Tokyo, Japan) (Hillegass et al., 2011) or PBS once a day between P13 and P16. At the P17, mice were sacrificed and enucleated. Enucleated eyes were fixed for 15 min in 4% PFA (paraformaldehyde) in PBS. Retinae were post-fixed for 1 h in 4% PFA in PBS after retinal wholemounts were isolated. Then, retinal wholemounts were stained with isolectin GS-IB4 from *Griffonia simplicifolia* conjugated to Alexa Fluor 594 (Fig. 1B). We measured the number of pixels in vaso-obliteration and neovascular tufts using the lasso tool and the magic wand tool of Photoshop, respectively (Adobe, San Jose, CA, USA) (Connor et al., 2009).

2.3. Real-time PCR

Total RNA was extracted from control and OIR mouse retinae and RT-PCR was performed using ReverTra Ace® qPCR RT Master Mix (TOYOBO, Osaka, Japan). Real-time PCR was performed using THUNDERBIRD® SYBR® qPCR Mix (TOYOBO). The primer sequences were as follows: HIF-1α forward GGTTCCAGCAGACCCAGTTA, HIF-1α reverse AGGCTCCTTGGATGAGCTTT, VEGF forward CCTGGTGGACATCTTCC AGGAGTACC, VEGF reverse GAAGCTCATCTCTCCTATGTGCTGGC, PDK1 forward GGCGGCTTTGTGATTTGTAT, PDK1 reverse ACCTGAA TCGGGGGATAAAC, BNIP3 forward GCTCCCAGACACCACAAGAT, BNIP3 reverse TGAGAGTAGCTGTGCGCTTC, HIF-2α forward TAAAG CGGCAGCTGGAGTAT, HIF-2α reverse ACTGGGAGGCATAGCACTGT, EPO forward CCTCATCTGCGACAGTCGAG, EPO reverse ACAACCCAT CGTGACATTTTCT, IGFBP3 forward CCAGGAAACATCAGTGAGTCC, IGFBP3 reverse GGATGGAACTTGGAATCGGTCA, APO2 forward CAG CCACGGTCAACAACTC, APO2 reverse CTTCTTTACGGATAGCAACC GAG.

2.4. Electroretinography and topotecan administration

The OIR procedure and administration of topotecan were performed as described above and electroretinography was conducted on P17. Electroretinography procedure was performed as previously reported (Jiang et al., 2018). Full field flash ERG responses were recorded using a Ganzfeld dome, an acquisition system, and LED stimulators (PuREC, MAYO, Inazawa, Japan). Following overnight dark adaptation, mice were anesthetized with a combination of midazolam, medetomidine and butorphanol tartrate (MMB) under a dim red light. A mixed solution of 0.5% tropicamide and 0.5% phenylephrine (Santen Pharmaceutical, Osaka, Japan) was used to dilate the pupils. The active electrodes were recorded with contact lens electrodes and a reference electrode was placed subcutaneously between the eyes. A clipping electrode to the tail served as a ground. ERG responses were obtained from both eyes of each animal. Scotopic responses were recorded under dark adaptation with various stimulus. Photopic responses were recorded with various stimulus under a white background (30 cd/m^2). For the quantification of a- and b-waves, the responses were processed by 30 Hz low pass filter. The amplitude of a-wave was measured from the baseline to the lowest point of a-wave. The amplitude of b-wave was measured from the lowest point of a-wave to the peak of b-wave. All mice were kept warm during the procedure using heat pads.

2.5. Luciferase assay

Murine cone photoreceptor cell line 661 W were transfected HIF-luciferase reporter gene construct (Cignal Lenti HIF Reporter, Qiagen, Venlo, Netherlands) to monitor HIF transcriptional activity. The HIF-luciferase construct encodes firefly luciferase gene under the control of hypoxia response element which binds HIFs. These cells were also co-transfected with CMV-renilla luciferase construct as an internal control. Cobalt chloride ($CoCl_2$, 200 μM, cobalt (II) chloride hexahydrate, Wako, Japan) was administrated to the cells in order to induce normoxic HIF activation 24 h before measuring the luminescence. To evaluate the suppressive effect of topotecan against HIF activation, topotecan (1 μM) (Patankar et al., 2013) was added at the same time as $CoCl_2$ was added. HIF inhibitory effect of topotecan on cells cultured in a hypoxic environment was also evaluated. 96-well plates seeded with the cells were placed in an incubator set at 3% oxygen. Topotecan was added just before entering the incubator. The luminescence was measured after culturing for 24 h in a low oxygen environment. The luminescence was measured with Dual-Luciferase® Reporter Assay System (Promega, Fitchburg, WI, USA).

2.6. Western blotting

Retinae were placed into lysis buffer. The composition of the lysis buffer is 10 mmol/l Tris-HCl, 100 mmol/l NaCl, 1 mmol/l EDTA, 1% Triton X-100, protease inhibitors. Each sample was fractionated by SDS-PAGE and transferred to polyvinylidene fluoride (PVDF) membranes. The membranes were blocked with 5% skim milk for 1 h at room temperature. The membranes were then incubated at 4 °C with rabbit monoclonal antibodies against HIF-1α (1:1500, Cell Signaling Technology), rabbit polyclonal antibodies against HIF-2α (1:1500, Novus Biologicals) or mouse monoclonal antibodies against β-actin (1:10000, Sigma). Finally, the membranes were incubated for 1 h at room temperature with a 1:3000 dilution of horseradish peroxidase-labeled secondary antibody for HIF-1α and HIF-2α or with a 1:15000 dilution of horseradish peroxidase-labeled secondary antibody for β-actin. The signals were detected using EzWestLumi plus chemiluminescent detection reagent (ATTO Corp.). Protein bands were visualized with chemiluminescence (ImageQuant LAS 4000 mini, GE Healthcare).

2.7. Optical coherence tomography (OCT)

OCT procedure was performed as previously reported using an SD-OCT system (Envisu R4310, Leica, Germany) at P17 (Jiang et al., 2018). Retinae were analyzed circumferentially at 500 μm from the optic nerve head. The retinal thickness was measured at arbitrary three points avoiding retinal neovascularization. The average of the results was taken as the retinal thickness of the individual mouse.

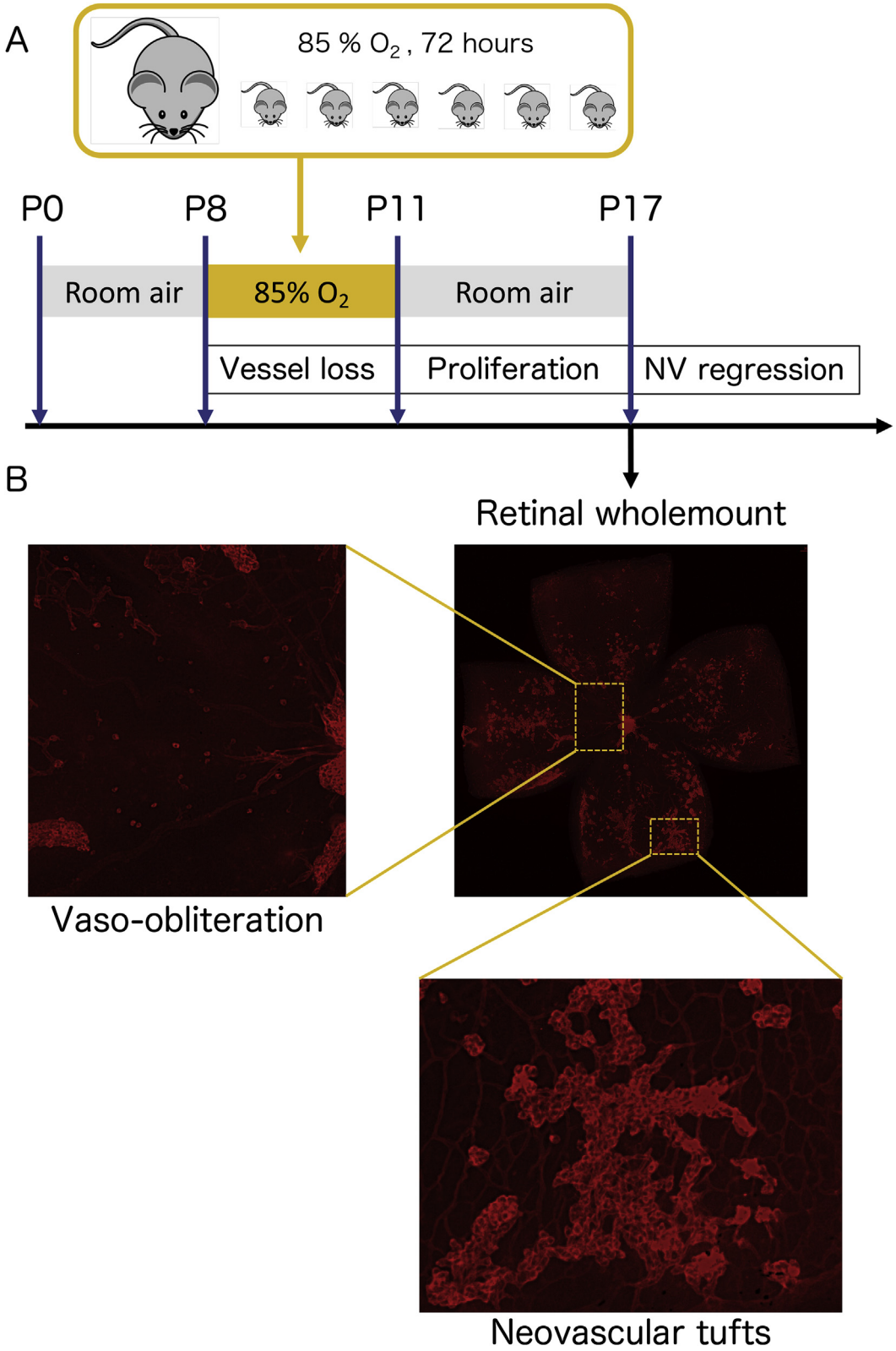

Fig. 1. Oxygen-induced retinopathy procedure.
(A) Postnatal day 8 (P8) mice were exposed to hyperoxia (85%) for 72 h. After the oxygen exposure, mice were placed back in room air until P17. (B) At P17, mice were sacrificed, and the eye balls were enucleated. Retinal wholemounts were stained with isolectin B4.

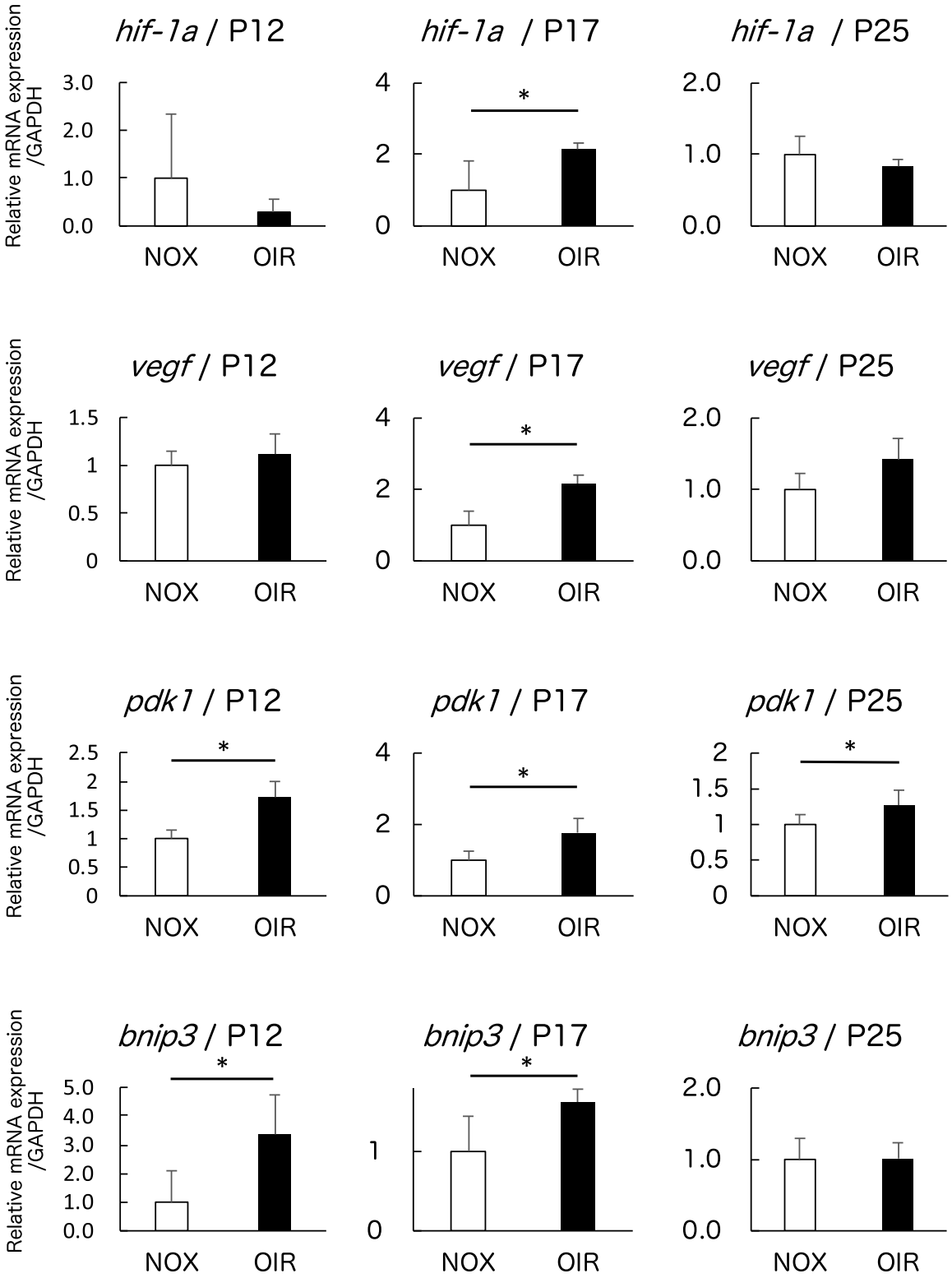

Fig. 2. mRNA expression of *hif-1α* and HIF target genes.
Retinae from mice bred at normoxia (NOX) and OIR at P12, P17, P25 were collected (n = 6, respectively). *hif-1α* and HIF related gene expression detected by real-time PCR. Note that these genes were significantly upregulated at P17, the proliferative period of OIR ($p < 0.05$). *$p < 0.05$. Error bars indicate mean plus s.d.

2.8. Statistical analyses

We used a two-tail Student's *t*-test for comparison of 2 groups and a one-way factorial ANOVA for the comparison of 3 groups, respectively. Probability values less than 0.05 were considered statistically significant. All results in this paper were expressed as the mean ± standard deviation.

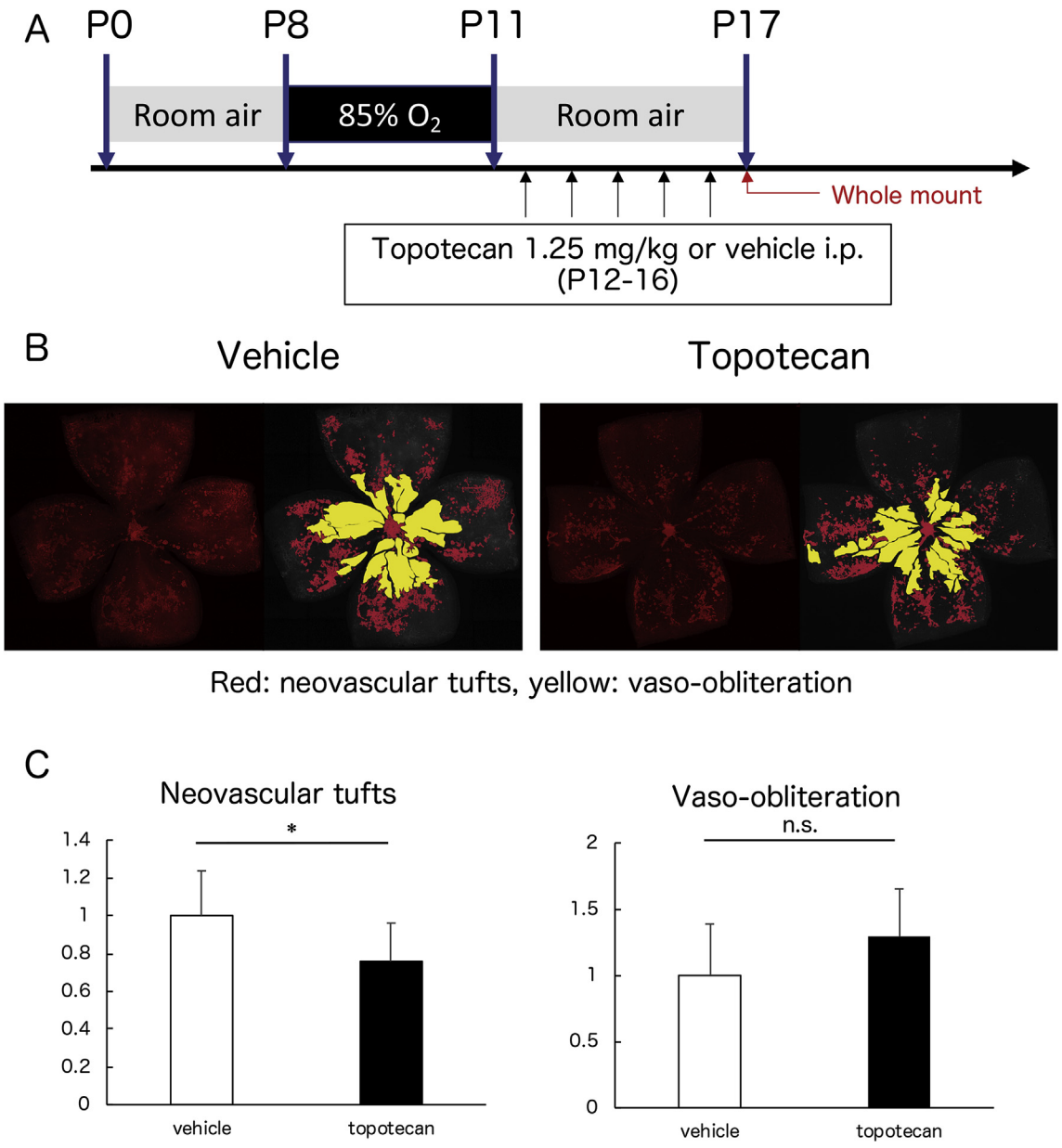

Fig. 3. Topotecan suppresses neovascularization of the murine OIR model.
(A) Vehicle (n = 9) or Topotecan (1.25 mg/kg, n = 10) were administrated intraperitoneally. (B) Representative image of retinal wholemount staining for isolectin B4. (C) Quantification of neovascular tufts (left) and vaso-obliteration (right) in OIR. Note that topotecan significantly suppressed neovascular tufts ($p < 0.05$) whereas no significant difference was observed in vaso-obliteration. *$p < 0.05$. Error bars indicate mean plus s.d.

3. Results

3.1. Expression of hif-1α and HIF target genes were upregulated during the latter stage of the proliferative period in OIR

To investigate expression pattern of *hif-1α* and HIF related genes such as *vegf*, *pdk1*, and *bnip3* during the OIR procedure, real-time PCR was performed. Retinae from mice bred at normoxia (NOX) and OIR at P12, P17, P25 were collected (n = 6, respectively). The expression of *hif-1α* and HIF related genes were significantly upregulated at P17 ($p < 0.05$) (Fig. 2).

3.2. Topotecan suppresses neovascularization in the murine OIR model

To evaluate neovascular tufts and vaso-obliteration area in OIR, we analyzed the retinal wholemount staining. Vehicle (n = 9) or topotecan (1.25 mg/kg, n = 10) were intraperitoneally administrated as the schedule shown in Fig. 3A. Administration of topotecan significantly suppressed neovascular tufts compared to vehicle injection ($p < 0.05$). No significant difference was observed in vaso-obliteration (Fig. 3B and C).

3.3. Topotecan prevents impaired visual function in the murine OIR model

We performed electroretinography and found that topotecan had protective effects on *impaired visual function* in OIR (Fig. 4A–D). In the dark-adapted a-waves, the amplitude was not changed, but the implicit time was significantly prolonged in OIR compared to normoxia controls ($p < 0.001$) (Fig. 4B). In both dark- and light-adapted b-waves, the amplitude was significantly reduced in OIR and administration of topotecan significantly suppressed the reduction of the amplitude (Fig. 4B and D). The implicit time of light-adapted b-waves were significantly

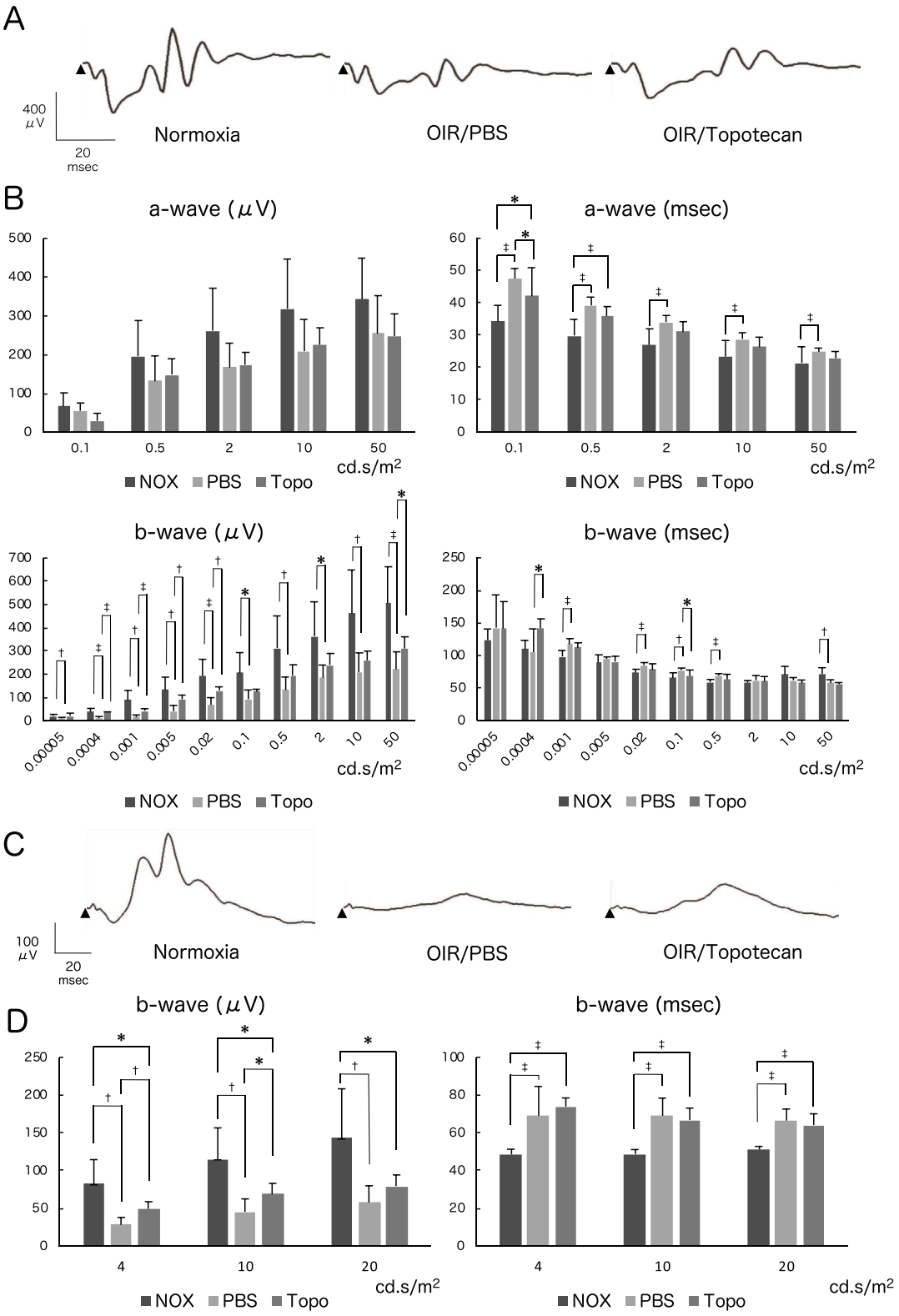

Fig. 4. Topotecan prevents the impaired visual function of the murine OIR model.
(A) Representative waveforms of the dark-adapted ERG performed at P17. (B) Quantification of amplitude (upper left) and implicit time (upper right) of a-wave, and amplitude (lower left) and implicit time (lower right) of b-wave. Note that topotecan significantly suppressed the reduced amplitude of b-wave in OIR. (C) Representative waveforms of the light-adapted ERG performed at P17. (D) Quantification of amplitude (left) and implicit time (right) of b-wave. Note that topotecan significantly suppressed the amplitude reduction. Arrowheads indicate light stimulus. *$p < 0.05$, †$p < 0.01$, ‡$p < 0.001$. Error bars indicate mean plus s.d.

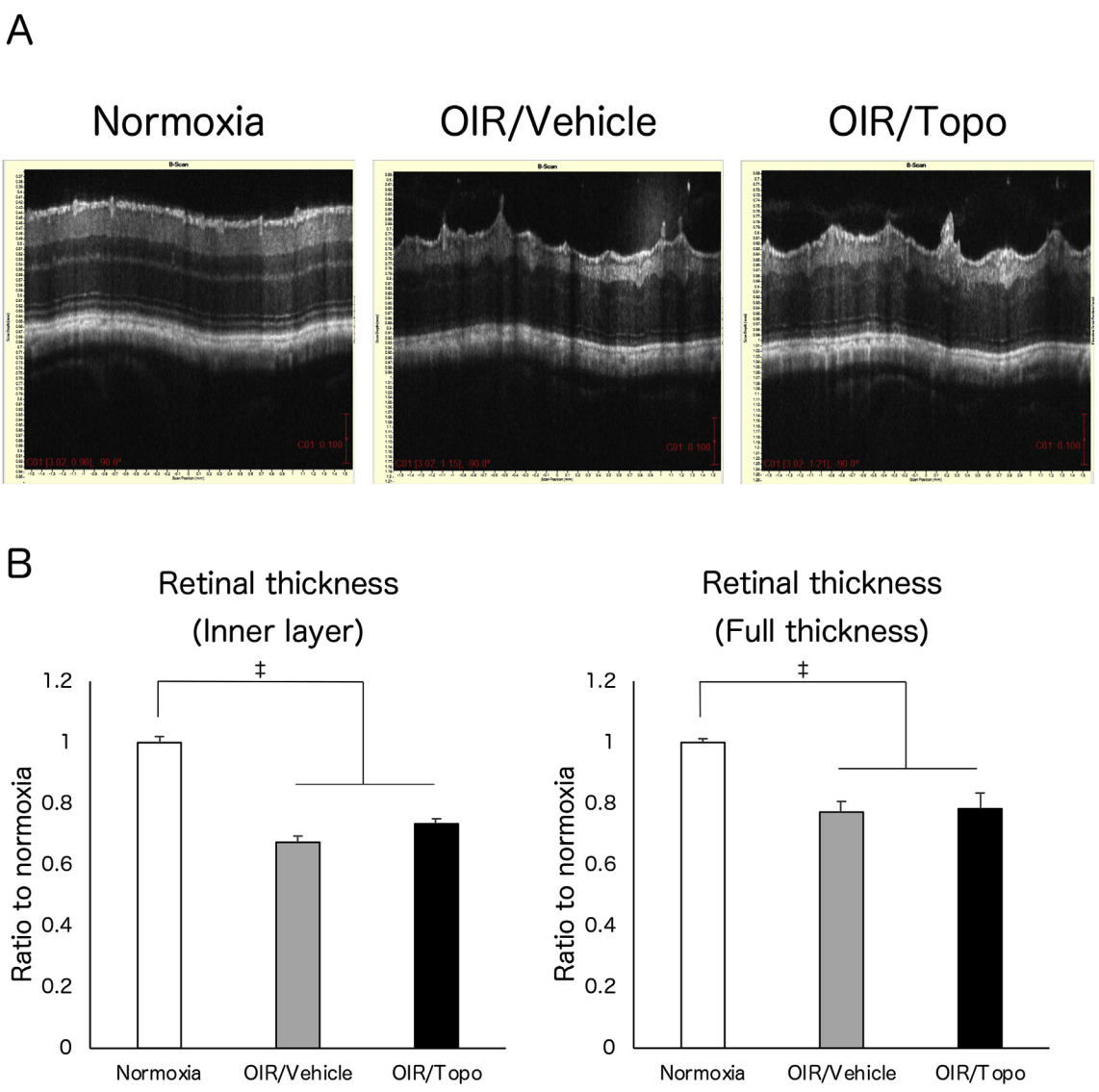

Fig. 5. Topotecan does not affect the retinal thickness decreased in OIR.
(A) Representative OCT images from each group of Normoxia (n = 8), OIR/Vehicle(n = 5), or OIR/Topotecan (n = 4) at P17. (B) Retinal thickness was significantly decreased in the OCT procedure while topotecan does not affect the retinal thickness. $^{‡}p < 0.001$. Error bars indicate mean plus s.d.

prolonged in OIR (Fig. 4D).

3.4. Topotecan does not affect the retinal thickness in the murine OIR model

In order to evaluate the morphological change of the retina by topotecan administration, we conducted experiments using OCT (Fig. 5A). Retinal thickness was measured for the inner layer and the full thickness. Administration of topotecan showed no significant effect on retinal thickness decreased in the OIR procedure (Fig. 5B).

3.5. Topotecan inhibits hif-1α and HIF target genes

In order to determine the mechanism of action of topotecan in the murine OIR model, upregulated genes at P17 in OIR such as *hif-1α*, *vegf*, *pdk1* and *bnip3* was compared with vehicle or topotecan administration. In the retinae of mice administered topotecan, *vegf* gene expression was significantly downregulated compared to vehicle-injected controls. On the other hands, gene expression of *hif-1α* showed a significant increase with topotecan administration possibly due to a negative feedback. Gene expression of *pdk1* and *bnip3* was not changed significantly by topotecan administration (Fig. 6A). To further explore the mechanism of topotecan, we evaluated several other hypoxia-related gene expression. The gene expression of *hif-2α* showed no significant change. On the other hands, the gene expression of *epo*, *igfbp3* and *apo2* were significantly upregulated in OIR. *apo2* was significantly suppressed, and *epo* and *igfbp3* tended to be suppressed by topotecan administration (Fig. 6B). Western blotting showed that the increased protein level of HIF-1α but not HIF-2α was suppressed by topotecan administration (Fig. 6C). Then, a luciferase assay was performed using 661 W cells to confirm the HIF inhibitory effect of topotecan *in vitro*. Administration of topotecan significantly inhibited HIF activity induced by hypoxia or cobalt chloride stabilizing HIF-αs (Fig. 6D).

3.6. Doxorubicin suppresses neovascularization in the murine OIR model

To evaluate neovascular tufts and vaso-obliteration area in OIR treated with another HIF inhibitor doxorubicin, we analyzed the retinal wholemount staining. Vehicle (n = 6) or doxorubicin (1 mg/kg, n = 6) were intraperitoneally administrated as the schedule shown in Fig. 7A. Administration of doxorubicin significantly suppressed neovascular tufts compared to vehicle injection ($p < 0.05$). No significant difference was observed in vaso-obliteration (Fig. 7B and C).

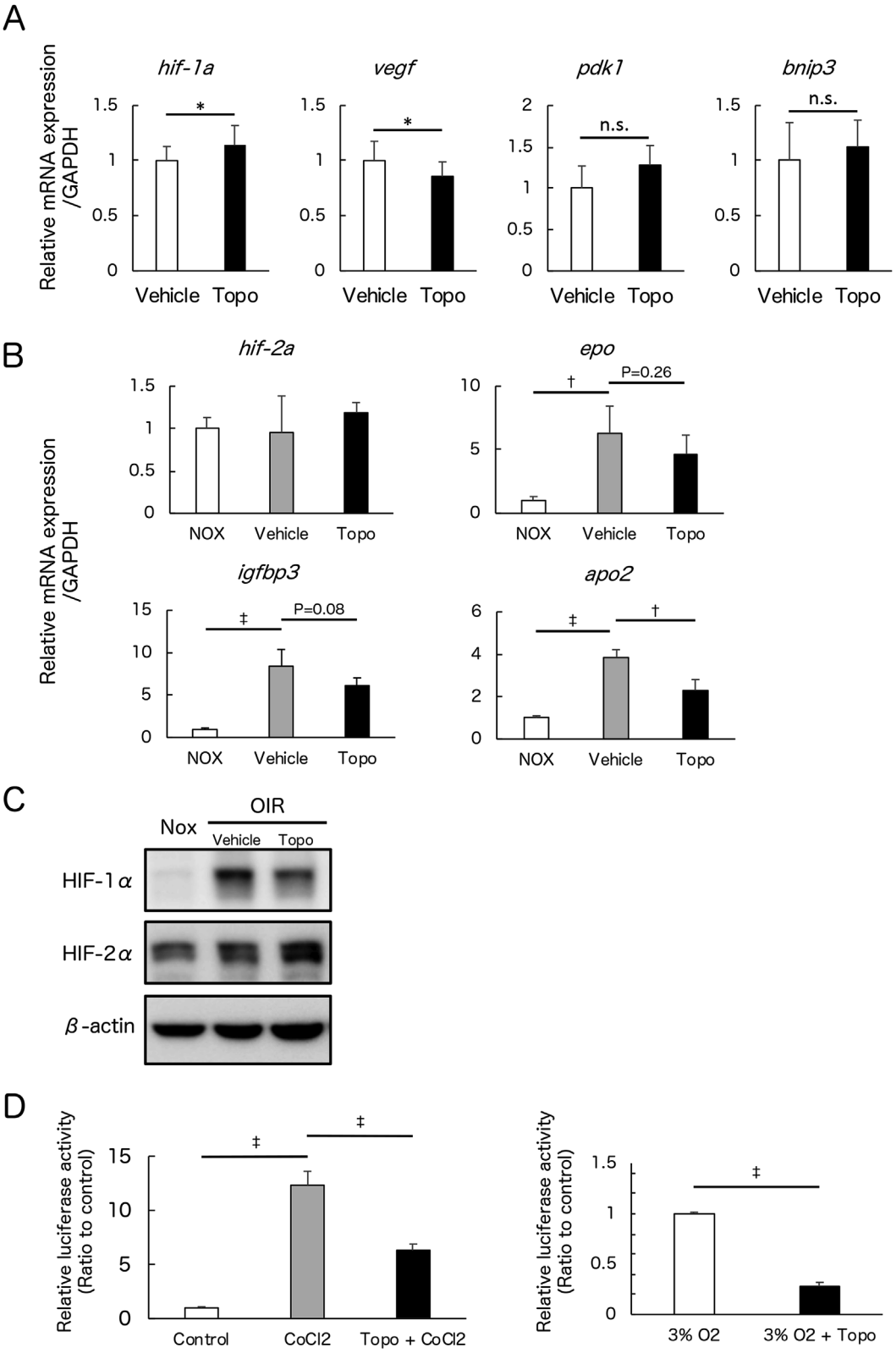

Fig. 6. Topotecan inhibits HIF-1α and HIF target genes.
(A) Retinae were extracted from the OIR mice on the P17 after administration of vehicle or topotecan. Real-time PCR was performed for *hif-1α*, *vegf*, *pdk1* and *bnip3*. Note that *hif-1α* was upregulated and *vegf* was downregulated significantly by topotecan administration at P17. Topotecan had no significant effect for *pdk1* and *bnip3*. (B) Retinae were collected from mice bred at normoxia (NOX) or OIR condition with vehicle or topotecan treatment at P17. *hif-2α, epo*, *igfbp3* and *apo2* gene expression were detected by real-time PCR. Note that gene expression of *hif-2α* showed no significant change and *epo*, *igfbp3* and *apo2* showed significantly upregulated in OIR. *apo2* was significantly suppressed and *epo* and *igfbp3* tended to be suppressed by topotecan administration. (C) Western blotting was performed for HIF-1α and HIF-2α with retinae from mice bred at NOX or OIR with vehicle or topotecan treatment at P17. Note that HIF-1α and HIF-2α were increased in OIR while HIF-1a was suppressed by topotecan administration. (D) HIF-reporter luciferase assay performed using 661 W cells. Note that topotecan significantly inhibited HIF activity induced by cobalt chloride and hypoxia. *$p < 0.05$, †$p < 0.01$, ‡$p < 0.001$. Error bars indicate mean plus s.d.

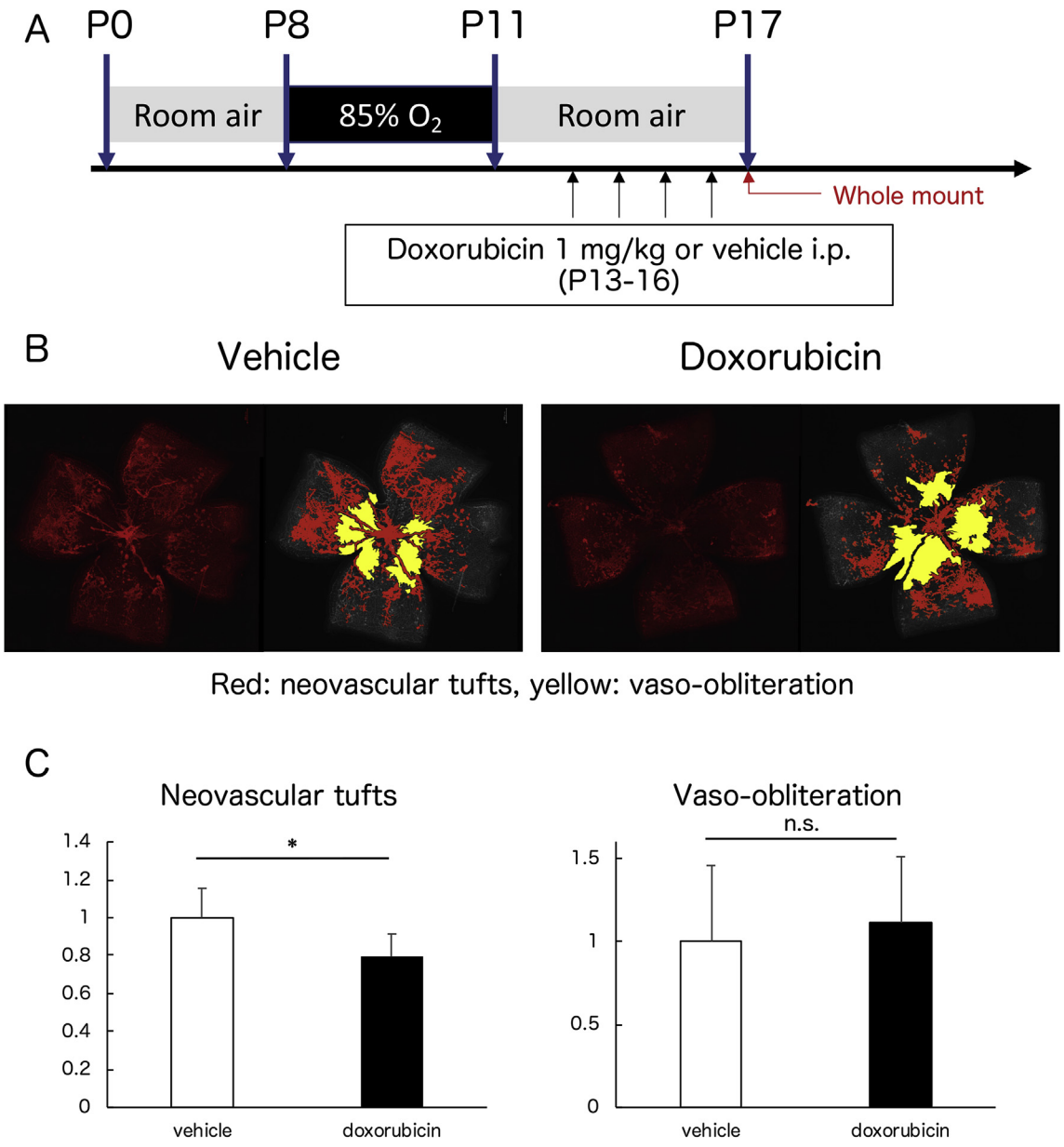

Fig. 7. Doxorubicin suppresses pathological neovascularization in the murine OIR model.
(A) Vehicle (n = 6) or doxorubicin (1 mg/kg, n = 6) were administrated intraperitoneally. (B) Representative image of retinal wholemount staining for isolectin B4. (C) Quantification of neovascular tufts (left) and vaso-obliteration (right) in OIR. Note that doxorubicin significantly suppressed neovascular tufts ($p < 0.05$) whereas no significant difference was observed in vaso-obliteration. *$p < 0.05$. Error bars indicate mean plus s.d.

4. Discussion

Several studies have been conducted on the effect of HIF inhibitors on ocular neovascularization to date (Gholipour et al., 2015; Sears et al., 2008; Zeng et al., 2017). Gholipour et al. has shown that intravitreal injection of topotecan prevented laser-induced choroidal neovascularization (CNV) in rats. Zeng et al. reported that inhibition of HIFαs using acriflavine has a preventive effect against retinal neovascularization in the murine OIR and laser-CNV model. In this study, we found that inhibition of HIFαs not only suppresses retinal neovascularization but also improves the impaired visual function that occurs with retinal neovascularization (Figs. 3 and 4).

HIFαs are involved with not only pathological retinal neovascularization but also normal retinal vessel formation in the developmental stage (Nakamura-Ishizu et al., 2012). Therefore, the effect of HIFαs modulation on young mice may vary considerably depending on when treatments are done. Jonathan Sears's group reported that the stabilization of HIFαs suppressed the angiogenesis of the murine OIR model (Sears et al., 2008). They reported that the inhibitory effect on angiogenesis was confirmed by administration of PHD inhibitor dimethyloxaloylglycine (DMOG) to mice at the time of exposure to hyperoxia. In contrast, the present study showed that inhibiting HIFαs after placing back to room air had an inhibitory effect on pathological retinal neovascularization (Figs. 3 and 7).

It has been reported that Müller cell-specific *hif-1α* knockout mice showed a significant decrease of neovascular tufts in OIR (Lin et al., 2011). In contrast, OIR-mediated neovascular tufts were decreased in astrocyte-specific *hif-2α* but not *hif-1α* knockout mice (Weidemann et al., 2010). Since HIF-1α is dominantly expressed and functioning in the sensory retina (Kurihara et al., 2010), we evaluated topotecan known as a HIF-1α inhibitor and confirmed that pharmacological HIF-1α inhibition is sufficient for a significant suppression against

pathological retinal neovascularization in OIR (Figs. 3 and 6).

Topotecan prevented pathological retinal neovascularization and impaired visual function (Figs. 3 and 4). We found that both HIF-1α and HIF-2α were increased at the protein level in OIR, and topotecan suppressed HIF-1α but not HIF-2α (Fig. 6C). Since topotecan is a topoisomerase 1 inhibitor as well as a HIF inhibitor, it may block other transcriptional factors (Onnis et al., 2009). Therefore, in order to confirm the pharmacological protection against HIF-mediated damage, we conducted another experiment using doxorubicin having a different HIF inhibition mechanism from topotecan. As a result, doxorubicin also prevented pathological retinal neovascularization (Fig. 7).

Topotecan significantly inhibited HIF activity induced by CoCl2 or hypoxia *in vitro* (Fig. 5D), and increased *hif-1α* but not *hif-2α* mRNA in vivo presumably due to a negative feedback (Fig. 5A and B). The expression of *pdk-1* and *bnip3* mRNA were significantly increased in OIR (Fig. 2) whereas no significant change in these gene expression was observed by administration of topotecan (Fig. 5A). On the other hands, angiogenesis-related genes such as *vegf*, *epo*, *igfbp3,* and *apo2* were significantly increased in OIR (Fig. 5B), and administration of topotecan showed a significant suppression of *vegf* and *apo2*, and a suppression tendency of *epo* and *igfbp3* (Fig. 5A and B). These data indicated that topotecan showed an inhibitory effect for pathological retinal neovascularization suppressing these HIF-mediated angiogenesis genes.

An improvement of visual function was observed in ERG by topotecan administration (Fig. 4). On the other hands, the morphological change was not observed (Fig. 5). Thus, the improvement effect of topotecan against the impaired visual function in OIR may be due to the improved vasculature and hence better blood flow. The implicit time of the dark-adapted b-waves of each group was not consistent (Fig. 4B). Thus, further electrophysiological examination is necessary to interpret the results.

In clinical studies, it has been reported that long-term anti-VEGF therapy may lead photoreceptor and retinal pigment epithelium (RPE) cell atrophy (Grunwald et al., 2014, 2017; Maguire et al., 2016). Furthermore, we previously reported that *Vegf* gene deletion in retinal pigment epithelium (RPE) cells induced choroidal and photoreceptor degeneration (Kurihara et al., 2012, 2016). Tokunaga et al. reported that an administration of VEGF inhibitor aflibercept reduced neovascular tufts and increased vaso-obliteration significantly in OIR (Tokunaga et al., 2014). They also showed that the VEGF inhibitor significantly decreased the amplitude of ERG. Their data suggest that VEGF antagonism may suppress physiological vascular development resulting in neurodegeneration. These results suggested that another target in addition to VEGF antagonism is now expected to treat neovascular ocular diseases.

In contrast to *Vegf* conditional knockout mice, adult-onset genetically *Hif*-inactivated mice showed no physiological disturbance (Kurihara et al., 2012) while pathological choroidal and retinal angiogenesis was suppressed in these mice (Kurihara et al., 2012, 2016; Weidemann et al., 2010). The current study showed that an administration of the HIF inhibitor could prevent pathological but not physiological angiogenesis. We also found topotecan is protective on visual function. This might be the results of retinal neovascular inhibition without disturbing the homeostasis (Liang et al., 2012). The therapeutic effect of the HIF inhibitor may support the potential to complement or alternate the present anti-VEGF therapy. Most of known HIF inhibitors including topotecan are classified as anticancer agents and these drugs may have adverse reactions both locally and systemically. Therefore, it is needed to explore safer HIF inhibitors in the future for clinical application.

5. Conclusions

In conclusion, our results propose that pharmacological HIF inhibition could be a therapeutic target of retinal neovascular and neurogenerative diseases.

Conflicts of interest

The authors declare no conflict of interest.

Acknowledgement

We thank H. Torii; S. Ikeda; Y. Hagiwara; Y. Tomita; Y. Katada; K. Mori; H. Kunimi; E. Yotsukura; M. Ibuki; N. Ozawa; Y. Wang; Y. Arita; A. Ishida and K. Takahashi for critical discussions. This work was supported by Grants-in-Aid for Scientific Research (KAKENHI, number 15K10881 and 18K09424) from the Ministry of Education, Culture, Sports, Science and Technology, JAPAN (MEXT) to Toshihide Kurihara.

References

Aiello, L.P., Pierce, E.A., Foley, E.D., Takagi, H., Chen, H., Riddle, L., Ferrara, N., King, G.L., Smith, L.E., 1995. Suppression of retinal neovascularization in vivo by inhibition of vascular endothelial growth factor (VEGF) using soluble VEGF-receptor chimeric proteins. Proc. Natl. Acad. Sci. U. S. A. 92, 10457–10461.

Cheung, N., Wong, I.Y., Wong, T.Y., 2014. Ocular anti-VEGF therapy for diabetic retinopathy: overview of clinical efficacy and evolving applications. Diabetes Care 37, 900–905.

Comparison of Age-related Macular Degeneration Treatments Trials Research, Group, Maguire, M.G., Martin, D.F., Ying, G.S., Jaffe, G.J., Daniel, E., Grunwald, J.E., Toth, C.A., Ferris 3rd, F.L., Fine, S.L., 2016. Five-Year outcomes with anti-vascular endothelial growth factor treatment of neovascular age-related macular degeneration: the comparison of age-related macular degeneration treatments trials. Ophthalmology 123, 1751–1761.

Connor, K.M., Krah, N.M., Dennison, R.J., Aderman, C.M., Chen, J., Guerin, K.I., Sapieha, P., Stahl, A., Willett, K.L., Smith, L.E., 2009. Quantification of oxygen-induced retinopathy in the mouse: a model of vessel loss, vessel regrowth and pathological angiogenesis. Nat. Protoc. 4, 1565–1573.

de Jong, P.T., 2006. Age-related macular degeneration. N. Engl. J. Med. 355, 1474–1485.

Ding, J., Wong, T.Y., 2012. Current epidemiology of diabetic retinopathy and diabetic macular edema. Curr. Diabetes Rep. 12, 346–354.

Ferrara, N., Gerber, H.P., LeCouter, J., 2003. The biology of VEGF and its receptors. Nat. Med. 9, 669–676.

Ferrara, N., Kerbel, R.S., 2005. Angiogenesis as a therapeutic target. Nature 438, 967–974.

Gholipour, M.A., Kanavi, M.R., Ahmadieh, H., Aldavood, S.J., Nourinia, R., Hosseini, S.B., Daftarian, N., Nashtaei, E.M., Tousi, A., Safi, S., 2015. Intravitreal topotecan inhibits laser-induced choroidal novascularization in a rat model. J. Ophthalmic Vis. Res. 10, 295–302.

Grunwald, J.E., Daniel, E., Huang, J., Ying, G.S., Maguire, M.G., Toth, C.A., Jaffe, G.J., Fine, S.L., Blodi, B., Klein, M.L., Martin, A.A., Hagstrom, S.A., Martin, D.F., Group, C.R., 2014. Risk of geographic atrophy in the comparison of age-related macular degeneration treatments trials. Ophthalmology 121, 150–161.

Grunwald, J.E., Pistilli, M., Daniel, E., Ying, G.S., Pan, W., Jaffe, G.J., Toth, C.A., Hagstrom, S.A., Maguire, M.G., Martin, D.F., 2017. Incidence and growth of geographic atrophy during 5 Years of comparison of age-related macular degeneration treatments trials. Ophthalmology 124, 97–104.

Guichard, S., Montazeri, A., Chatelut, E., Hennebelle, I., Bugat, R., Canal, P., 2001. Schedule-dependent activity of topotecan in OVCAR-3 ovarian carcinoma xenograft: pharmacokinetic and pharmacodynamic evaluation. Clin. Cancer Res. 7, 3222–3228.

Hillegass, J.M., Blumen, S.R., Cheng, K., MacPherson, M.B., Alexeeva, V., Lathrop, S.A., Beuschel, S.L., Steinbacher, J.L., Butnor, K.J., Ramos-Nino, M.E., Shukla, A., James, T.A., Weiss, D.J., Taatjes, D.J., Pass, H.I., Carbone, M., Landry, C.C., Mossman, B.T., 2011. Increased efficacy of doxorubicin delivered in multifunctional microparticles for mesothelioma therapy. Int. J. Cancer 129, 233–244.

Jiang, X., Kurihara, T., Kunimi, H., Miyauchi, M., Ikeda, S.I., Mori, K., Tsubota, K., Torii, H., Tsubota, K., 2018. A highly efficient murine model of experimental myopia. Sci. Rep. 8, 2026.

Kaelin Jr., W.G., Ratcliffe, P.J., 2008. Oxygen sensing by metazoans: the central role of the HIF hydroxylase pathway. Mol. Cell 30, 393–402.

Kurihara, T., Kubota, Y., Ozawa, Y., Takubo, K., Noda, K., Simon, M.C., Johnson, R.S., Suematsu, M., Tsubota, K., Ishida, S., Goda, N., Suda, T., Okano, H., 2010. von Hippel-Lindau protein regulates transition from the fetal to the adult circulatory system in retina. Development 137, 1563–1571.

Kurihara, T., Westenskow, P.D., Bravo, S., Aguilar, E., Friedlander, M., 2012. Targeted deletion of Vegfa in adult mice induces vision loss. J. Clin. Investig. 122, 4213–4217.

Kurihara, T., Westenskow, P.D., Gantner, M.L., Usui, Y., Schultz, A., Bravo, S., Aguilar, E., Wittgrove, C., Friedlander, M., Paris, L.P., Chew, E., Siuzdak, G., Friedlander, M., 2016. Hypoxia-induced metabolic stress in retinal pigment epithelial cells is sufficient to induce photoreceptor degeneration. Elife 5, 14319.

Lains, I., Figueira, J., Santos, A.R., Baltar, A., Costa, M., Nunes, S., Farinha, C., Pinto, R., Henriques, J., Silva, R., 2014. Choroidal thickness in diabetic retinopathy: the influence of antiangiogenic therapy. Retina 34, 1199–1207.

Liang, X., Zhou, H., Ding, Y., Li, J., Yang, C., Luo, Y., Li, S., Sun, G., Liao, X., Min, W., 2012. TMP prevents retinal neovascularization and imparts neuroprotection in an oxygen-induced retinopathy model. Investig. Ophthalmol. Vis. Sci. 53, 2157–2169.

Lin, M., Chen, Y., Jin, J., Hu, Y., Zhou, K.K., Zhu, M., Le, Y.Z., Ge, J., Johnson, R.S., Ma,

J.X., 2011. Ischaemia-induced retinal neovascularisation and diabetic retinopathy in mice with conditional knockout of hypoxia-inducible factor-1 in retinal Muller cells. Diabetologia 54, 1554–1566.
Maguire, M.G., Martin, D.F., Ying, G.S., Jaffe, G.J., Daniel, E., Grunwald, J.E., Toth, C.A., Ferris 3rd, F.L., Fine, S.L., 2016. Five-Year outcomes with anti-vascular endothelial growth factor treatment of neovascular age-related macular degeneration: the comparison of age-related macular degeneration treatments trials. Ophthalmology 123, 1751–1761.
Mole, D.R., Blancher, C., Copley, R.R., Pollard, P.J., Gleadle, J.M., Ragoussis, J., Ratcliffe, P.J., 2009. Genome-wide association of hypoxia-inducible factor (HIF)-1alpha and HIF-2 alpha DNA binding with expression profiling of hypoxia-inducible transcripts. J. Biol. Chem. 284, 16767–16775.
Nakamura-Ishizu, A., Kurihara, T., Okuno, Y., Ozawa, Y., Kishi, K., Goda, N., Tsubota, K., Okano, H., Suda, T., Kubota, Y., 2012. The formation of an angiogenic astrocyte template is regulated by the neuroretina in a HIF-1-dependent manner. Dev. Biol. 363, 106–114.
Okabe, K., Kobayashi, S., Yamada, T., Kurihara, T., Tai-Nagara, I., Miyamoto, T., Mukouyama, Y.S., Sato, T.N., Suda, T., Ema, M., Kubota, Y., 2014. Neurons limit angiogenesis by titrating VEGF in retina. Cell 159, 584–596.
Onnis, B., Rapisarda, A., Melillo, G., 2009. Development of HIF-1 inhibitors for cancer therapy. J. Cell Mol. Med. 13, 2780–2786.
Ozaki, H., Yu, A.Y., Della, N., Ozaki, K., Luna, J.D., Yamada, H., Hackett, S.F., Okamoto, N., Zack, D.J., Semenza, G.L., Campochiaro, P.A., 1999. Hypoxia inducible factor-1alpha is increased in ischemic retina: temporal and spatial correlation with VEGF expression. Investig. Ophthalmol. Vis. Sci. 40, 182–189.
Patankar, N.A., Pritchard, J., van Grinsven, M., Osooly, M., Bally, M.B., 2013. Topotecan and doxorubicin combination to treat recurrent ovarian cancer: the influence of drug exposure time and delivery systems to achieve optimum therapeutic activity. Clin. Cancer Res. 19, 865–877.
Pieramici, D.J., Rabena, M.D., 2008. Anti-VEGF therapy: comparison of current and future agents. Eye 22, 1330–1336.
Rapisarda, A., Uranchimeg, B., Sordet, O., Pommier, Y., Shoemaker, R.H., Melillo, G., 2004. Topoisomerase I-mediated inhibition of hypoxia-inducible factor 1: mechanism and therapeutic implications. Cancer Res. 64, 1475–1482.
Resnikoff, S., Pascolini, D., Etya'ale, D., Kocur, I., Pararajasegaram, R., Pokharel, G.P., Mariotti, S.P., 2004. Global data on visual impairment in the year 2002. Bull. World Health Organ. 82, 844–851.
Sears, J.E., Hoppe, G., Ebrahem, Q., Anand-Apte, B., 2008. Prolyl hydroxylase inhibition during hyperoxia prevents oxygen-induced retinopathy. Proc. Natl. Acad. Sci. U. S. A 105, 19898–19903.
Smith, L.E., Wesolowski, E., McLellan, A., Kostyk, S.K., D'Amato, R., Sullivan, R., D'Amore, P.A., 1994. Oxygen-induced retinopathy in the mouse. Investig. Ophthalmol. Vis. Sci. 35, 101–111.
Tokunaga, C.C., Mitton, K.P., Dailey, W., Massoll, C., Roumayah, K., Guzman, E., Tarabishy, N., Cheng, M., Drenser, K.A., 2014. Effects of anti-VEGF treatment on the recovery of the developing retina following oxygen-induced retinopathy. Investig. Ophthalmol. Vis. Sci. 55, 1884–1892.
Uddin, M.I., Evans, S.M., Craft, J.R., Capozzi, M.E., McCollum, G.W., Yang, R., Marnett, L.J., Uddin, M.J., Jayagopal, A., Penn, J.S., 2016. In vivo imaging of retinal hypoxia in a model of oxygen-induced retinopathy. Sci. Rep. 6, 31011.
Wang, G.L., Semenza, G.L., 1995. Purification and characterization of hypoxia-inducible factor 1. J. Biol. Chem. 270, 1230–1237.
Weidemann, A., Krohne, T.U., Aguilar, E., Kurihara, T., Takeda, N., Dorrell, M.I., Simon, M.C., Haase, V.H., Friedlander, M., Johnson, R.S., 2010. Astrocyte hypoxic response is essential for pathological but not developmental angiogenesis of the retina. Glia 58, 1177–1185.
Yu, T., Tang, B., Sun, X., 2017. Development of inhibitors targeting hypoxia-inducible factor 1 and 2 for cancer therapy. Yonsei Med. J. 58, 489–496.
Zeng, M., Shen, J., Liu, Y., Lu, L.Y., Ding, K., Fortmann, S.D., Khan, M., Wang, J., Hackett, S.F., Semenza, G.L., Campochiaro, P.A., 2017. The HIF-1 antagonist acriflavine: visualization in retina and suppression of ocular neovascularization. J. Mol. Med. (Berl) 95, 417–429.